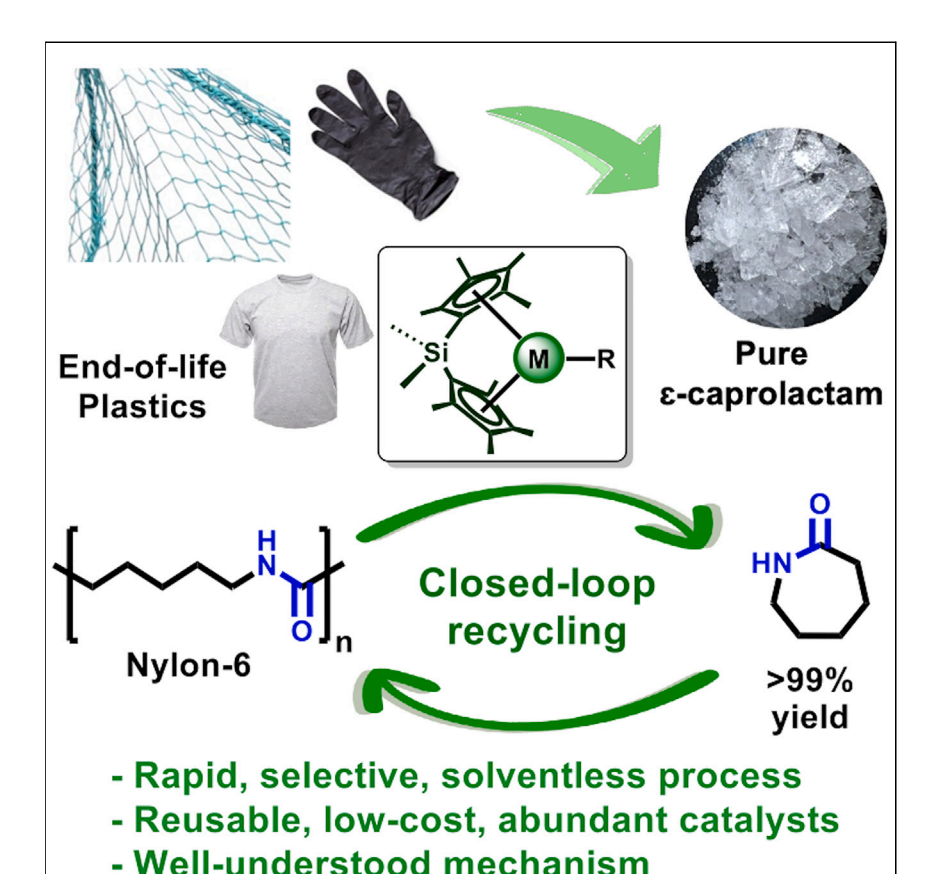
Chem



### **Article**

# Catalyst metal-ligand design for rapid, selective, and solventless depolymerization of Nylon-6 plastics



Nylon-6 is an extraordinarily robust material that lacks biodegradability, leading to persistence and accumulation in the environment. In this mechanism-oriented catalysis study, we design an efficient, tunable metallocene catalytic system using abundant metals, achieving a record Nylon-6 depolymerization rate with  $\geq$  99% yield of re-polymerizable  $\epsilon$ -caprolactam. This solventless process operates with a minimal 0.04 mol % catalyst in a model continuous process. These catalysts and processes are compatible with depolymerizing diverse commodity Nylons, such as fishing nets, carpets, clothing, and plastic mixtures.

Liwei Ye, Xiaoyang Liu, Kristen B. Beckett, ..., Linda J. Broadbelt, Yosi Kratish, Tobin J.

broadbelt@northwestern.edu (L.J.B.) yosi.kratish@northwestern.edu (Y.K.) t-marks@northwestern.edu (T.J.M.)

#### Highlights

Rapid and selective Nylon-6 depolymerization catalyzed by a new metallocene-based system

Tunable catalytic structures enable effective and well-defined mechanisms

Mild depolymerization conditions using reusable, earth-abundant catalysts

Depolymerization of diverse endof-life Nylons catalyzed by stable ansa-complex





Ye et al., Chem 10, 172–189 January 11, 2024 © 2023 Elsevier Inc. https://doi.org/10.1016/j.chempr.2023.10.022







#### Article

# Catalyst metal-ligand design for rapid, selective, and solventless depolymerization of Nylon-6 plastics

Liwei Ye, <sup>1</sup> Xiaoyang Liu, <sup>2</sup> Kristen B. Beckett, <sup>1</sup> Jacob O. Rothbaum, <sup>1</sup> Clarissa Lincoln, <sup>3,4</sup> Linda J. Broadbelt,<sup>2,\*</sup> Yosi Kratish,<sup>1,\*</sup> and Tobin J. Marks<sup>1,5,\*</sup>

#### **SUMMARY**

Developing effective catalysis to address end-of-life Nylon pollution is urgent yet remains underdeveloped. Nylon-6 is a resilient synthetic plastic and a major contributor to ocean pollution. Here, we report a metallocene catalytic system based on earth-abundant early transition and lanthanide metals that mediates Nylon-6 depolymerization at unprecedented rates up to 810 (ε-caprolactam). mol(Cat.) $^{-1}$ ·h $^{-1}$  at 240°C in  $\geq$ 99% yield. This solventless process operates with catalyst loadings as low as 0.04 mol % at temperatures as low as 220°C—the mildest Nylon-6 depolymerization conditions reported to date. This metallocene catalysis can be carried out in a simulated continuous process, and the resulting  $\varepsilon$ -caprolactam can be re-polymerized to higher-quality Nylon-6. Experimental and DFT analyses identify effective depolymerization pathways involving catalytic intra-Nylon-chain "unzipping" assisted by  $\pi$ -ligand effects and inter-chain "hopping." A robust chelating ansa-yttrocene is particularly effective in depolymerizing diverse commodity end-of-life articles, such as fishing nets, carpets, clothing, and plastic mixtures.

#### INTRODUCTION

Catalysis is central to countless chemical transformations and in principle holds great promise for the efficient recycling of commodity plastics. 1-3 Plastics are versatile, low-cost materials that have dramatically enhanced the quality of life for more than a century. Currently, plastics are produced at an annual rate of 450 million tons, which is projected to double by 2045.<sup>4</sup> Nevertheless, with only limited tools available to address plastics end of life, their accumulation has emerged as a global environmental challenge. 5,6 For example, Nylon polyamides, which are produced on a scale exceeding 8.9 million tons annually, significantly contribute to the nondegradable plastic waste pollution in oceans and landfills, reflecting their outstanding chemical inertness and paucity of effective recycling technologies.8 Indeed, it is estimated that by 2050, plastic waste will outweigh fish in the ocean, with Nylon-6 contributing ca. 10% of ocean plastic pollution as discarded/lost fishing nets ("ghost nets"). 10 This amounts to >600,000 tons of abandoned fishing nets annually. 11,12 Furthermore, Nylons are the most prevalent polymers in the stomachs of marine animals, illustrating the persistence challenge to global marine ecosystems.<sup>13</sup>

Since its invention by Schlack in 1938, <sup>14</sup> Nylon-6 has emerged as a robust and versatile thermoplastic with widespread applications in the fishing, automotive,

#### THE BIGGER PICTURE

Nylon-6 is an extraordinarily robust and versatile polymer used for applications such as packaging, textiles, automotive parts, and fishing nets. It is produced at >5 megatons annually. Its environmental persistence has led to significant waste accumulations—discarded Nylon fishing nets comprise ca. 10% of ocean plastic, and producing new Nylon-6 has a high carbon footprint. In principle, catalytic chemical recycling of Nylon-6 to recover the starting monomer, ε-caprolactam, would be ideal, but the inertness of this plastic has hindered progress. Here, we report a rationally designed organometallic catalytic system using earth-abundant metals that achieves Nylon-6 depolymerization under mild and benign solvent-free conditions at unprecedented rates and selectivity. This process is effective for diverse commodity end-of-life articles such as fishing nets, carpets, clothing, and plastic mixtures.



## **Chem** Article



packaging, carpet, and textile industries<sup>15</sup> due to its high tensile strength, rigidity, toughness, as well as thermal and abrasion resistance.<sup>14–16</sup> Nylon-6 commercial products dominate the global Nylon market with more than 50% of the total revenue<sup>7</sup> and a market size projected to exceed \$21 billion by 2026.<sup>17,18</sup> Nevertheless, despite the importance of Nylon-6, end-of-life management of Nylon waste falls far behind the worldwide production rate.<sup>8,19,20</sup> Traditional approaches to partially recover the energy stored in plastic waste, such as incineration and pyrolysis, in the case of Nylons release toxic/harmful gases, including CO, NH<sub>3</sub>, and CO<sub>2</sub>, further exacerbating the environmental challenges.<sup>21</sup> In addition, mechanical recycling of Nylons causes substantial property degradation, reflecting the elevated required temperatures, and is considered economically less attractive.<sup>11,22</sup>

If efficient, chemical recycling of Nylon-6 would provide an attractive route to regenerate  $\varepsilon$ -caprolactam monomer, which is currently produced from fossil feedstocks and contributes significantly to greenhouse gas emissions. <sup>23,24</sup> Conventional catalytic depolymerization processes require elevated temperatures and high steam pressures. Kamimura and Yamamoto et al. reported Nylon-6 depolymerization in ionic liquids to produce  $\varepsilon$ -caprolactam in 55%–85% yields with 5 wt % 4-dimethylaminopyridine (DMAP) as the catalyst. <sup>25–27</sup> Note that this process requires temperatures above 300°C, ionic liquids that decompose at these temperatures, and DMAP, which is toxic. <sup>26,27</sup> In 2020, Milstein et al. reported a novel homogeneous Ru-catalyzed deconstruction of Nylons to linear amino alcohols via hydrogenation at 70 bar H<sub>2</sub> pressures and 48 h reaction times. <sup>28</sup> For Nylon-6, 24%–48% yields of 6-amino-1-hexanol were obtained (Figure 1A). <sup>28</sup>

We hypothesized that early transition metal and lanthanide complexes, which are highly electrophilic, kinetically labile with polar metal-ligand bonding, and are active/selective catalysts in diverse heteroatom hydro-functionalization and related C-N/C-O cleavage processes, <sup>29,30</sup> might function as effective Nylon-6 depolymerization catalysts. Note that the abundance of La and Y in the earth's crust is comparable to that of Co, Ni, and Cu<sup>31,32</sup> and that La and Y are 2,000× and 600× cheaper than Ru, respectively. <sup>33,34</sup> In terms of production-related global warming potential, La is 0.09%, 0.28%, and 0.52% of that of Pt, Pd, and Ru, respectively, whereas Y is 0.12%, 0.38%, and 0.72%, respectively. <sup>35</sup>

In early exploratory work, we investigated  $Ln(NTMS_2)_3$  (TMS = SiMe<sub>3</sub>) complexes for Nylon-6 depolymerization activity (Figures 1B and 2A) and found modest rates and yields that decline with decreasing lanthanide ionic radius (i.r.) (1, Figure 2B). Due to their low activities and partial volatility during reaction conditions, the  $Ln(NTMS_2)_3$  catalyst and Nylon-6 must be intimately mixed before and during the polymer melting stage. Thus,  $Ln(NTMS_2)_3$  is catalytically effective for virgin Nylon-6 powder, whereas Nylon yarn must be cryogenically milled even for moderate  $\epsilon$ -caprolactam rates and yields. Furthermore, the simple  $Ln(NTMS_2)_3$  tris-amido ligation offers little opportunity for mechanistic tuning, risks catalyst-polymer chain cross-linking/immobilization, and depolymerization rates are only tunable via the Ln i.r. Considering these limitations, we sought ligationally more tunable and less volatile catalysts in a mechanism-oriented approach.

Here, we report a new  $\pi$ -ligated class of metallocene catalysts, which are far more effective in Nylon-6 depolymerization with unprecedented turnover frequencies (TOFs) up to 810 ( $\epsilon$ -caprolactam)·mol(Cat.) $^{-1}$ ·h $^{-1}$  at 240°C (Figures 1C and 2B). It will be seen that these metallocene-mediated depolymerization processes proceed in high yields—up to 99% yield of recovered re-polymerizable caprolactam

<sup>&</sup>lt;sup>1</sup>Department of Chemistry and the Institute for Sustainability and Energy, Northwestern University, 2145 Sheridan Road, Evanston, IL 60208-3113. USA

<sup>&</sup>lt;sup>2</sup>Department of Chemical and Biological Engineering, and Institute for Sustainability and Energy, Northwestern University, 2145 Sheridan Road, Evanston, IL 60208-3113, USA

<sup>&</sup>lt;sup>3</sup>Renewable Resources and Enabling Sciences Center, National Renewable Energy Laboratory, Golden, CO 80401, USA

<sup>&</sup>lt;sup>4</sup>BOTTLE Consortium, National Renewable Energy Laboratory, Golden, CO 80401, USA

<sup>&</sup>lt;sup>5</sup>Lead contact

<sup>\*</sup>Correspondence: broadbelt@northwestern.edu (L.J.B.), yosi.kratish@northwestern.edu (Y.K.), t-marks@northwestern.edu (T.J.M.)





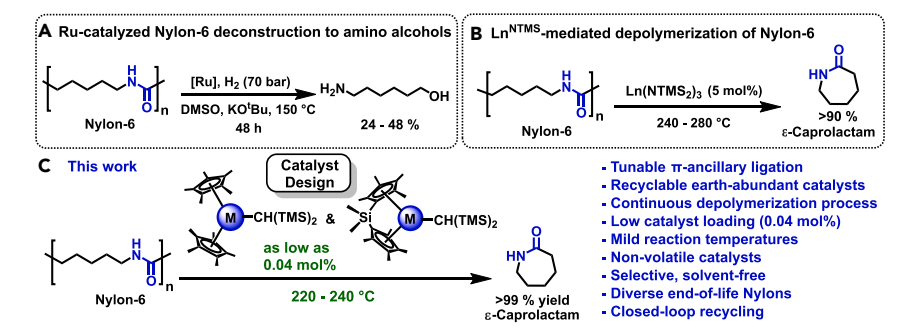


Figure 1. Recent examples of catalytic approaches to Nylon-6 chemical recycling.

monomer, operating under mild conditions—the lowest Nylon-6 to  $\varepsilon$ -caprolactam depolymerization temperature reported to date, 220°C, while employing catalyst loadings as low as 0.04 mol % and can operate in a model continuous process as opposed to a batch mode. Furthermore, it will be seen that the highly active and robust *ansa*-yttrocene complex 6 catalytically depolymerizes a wide variety of end-of-life Nylon articles and can be used to separate mixed plastic waste. Finally, the mechanism of this efficient catalytic depolymerization process is probed by experiment and by high-level free volume and density functional theory (DFT) computation.

#### **RESULTS AND DISCUSSION**

The benchmark catalyst  $Ln(NTMS_2)_3$  (1) is commercially available, and the metallocene catalysts were prepared and purified by literature procedures. <sup>37–39</sup> Finely powdered commercial virgin Nylon-6 ( $M_n = 14,800 \text{ g mol}^{-1}$ ) was first utilized to screen catalysts and catalytic conditions, to maximize polymer-catalyst contact, and to achieve uniform mixing/heating. All depolymerizations were performed in a green solventless batch mode, with crystalline  $\epsilon$ -caprolactam product collecting on the cold reactor wall (see supplemental information for details).

In attempts to lower catalyst 1 loading from the 5 mol % (90% yield; see prior work<sup>36</sup>) to 1 mol %, a moderate  $\varepsilon$ -caprolactam yield was obtained (69%, Table 1, entry 1) in 0.5 h reaction time/240°C using the present solventless methodology. Further

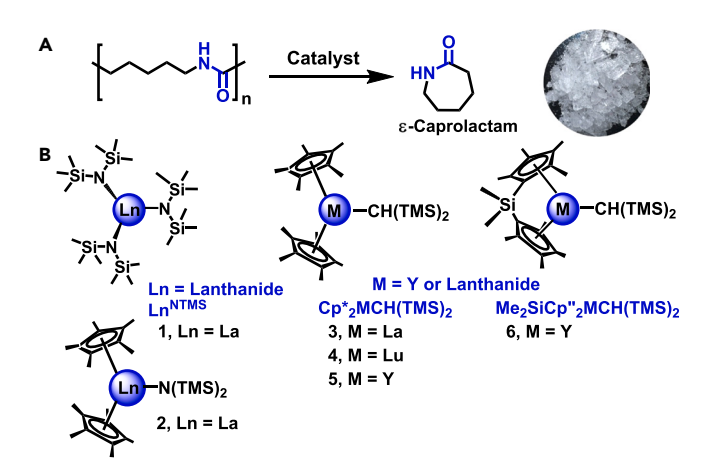


Figure 2. Depolymerization process and catalysts

(A) Nylon-6 depolymerization process presented in this study, producing crystalline caprolactam.

(B) Depolymerization catalysts are investigated here.  $TMS = SiMe_3$ .



Table 1. Optimization of the catalytic Nylon-6 depolymerization conditions shown in Figure 2A

Entry	Catalyst	Catalyst loading (mol %)	Time (h)	Temperature (°C)	Yield (%) <sup>b</sup>	TOF°
1				<u> </u>		
ļ	1	1.0	0.5	240	69	138
2	1	0.2	1.0	240	5.6	28.0
3	2	1.0	6.0	240	17	2.83
4	3	1.0	0.5	240	91	182
5	3	1.0	1.0	240	99 <sup>d</sup>	99.0
6	3	0.2	1.0	240	93	465
7	3	0.2	0.5	240	81	810
8 <sup>e</sup>	3	0.2	3.0	240	97 (94) <sup>f</sup>	162
9	3	1.0	2.0	220	90	45.0
10	3	0.2	4.0	220	95	119
11	1	0.2	24	220	2.4	0.50
12	4	1.0	1.0	240	24	24
13	5	1.0	1.0	240	2.2	2.2
14	5	5.0	24	240	93	0.78
15	6	1.0	1.0	240	94	94
16	6	1.0	2.0	240	>99	49.9

<sup>&</sup>lt;sup>a</sup>General depolymerization conditions: static vacuum (10<sup>-3</sup> Torr), 100 mg of Nylon-6 powder in a 50 mL Schlenk flask, unless otherwise stated.

lowering the catalyst loading to 0.2 mol % depressed the depolymerization yield to 5.6% (Table 1, entry 2), prompting catalyst ligand redesign to ensure monomeric character and to achieve higher activities and yields.

#### Catalyst ligand design

We envisioned constraining the  $Ln^{3+}$  coordination sphere using non-dissociable ancillary  $\pi$ -ligands to sterically shield the electrophilic  $Ln^{3+}$  centers while minimizing impediments to substrate approach. Thus,  $\pi$ -ligands such as bis(pentamethyl-cyclopentadienyl) (Cp\*2) (Figure 2B), which offer high coordinative stability, good solubility in organic media, and rich catalytic chemistry<sup>37</sup> were screened. Here, the  $La^{3+}$  coordination sphere was first modified by replacing two –TMS2N 1 active sites with Cp\* ligands, Cp\*2LaN(TMS)2 (2); however, this led to a reduced depolymerization activity under the present solventless conditions with 1 mol % catalyst and an extended reaction time (Table 1, entry 3), possibly reflecting inadequate La-NTMS2 basicity to initiate the depolymerization process, and was not investigated further.

Next,  $Cp^*_2LaCH(TMS)_2$  (3), which efficiently catalyzes C–N bond-forming reactions such as cyclohydroaminations, <sup>29,30</sup> was investigated for Nylon-6 depolymerization, which also requires intramolecular cyclization to form C–N bonds. Strikingly, 3 is a highly effective catalyst at 1 mol % loading, providing a 91% yield in only 0.5 h at 240°C (Table 1, entry 4). This represents a significant advance over  $Cp^*_2LaN(TMS)_2$ , revealing marked  $\sigma$ -bonded ligand effects on initiation, which are supported by DFT analysis (*vide infra*). Extending the reaction time to 1 h affords a 99% yield (Table 1, entry 5), which was performed in duplicate with a consistent result, reflecting good reproducibility of the metallocene catalysis. A 0.2 mol % loading of catalyst 3 provides a 93% yield (Table 1, entry 6), in marked contrast to catalyst 1 (5.6% yield). This depolymerization is found to reach 81% yield in only 0.5 h (Table 1, entry 7).

<sup>&</sup>lt;sup>b</sup>Yields determined by <sup>1</sup>H NMR with a mesitylene internal standard.

<sup>&</sup>lt;sup>c</sup>Turnover frequencies (TOFs) estimated in units of (mol  $\varepsilon$ -caprolactam)·(mol Cat.)<sup>-1</sup>·(h)<sup>-1</sup>.

<sup>&</sup>lt;sup>d</sup>This reaction was performed in duplicate, both trials providing the same yield.

eScaled-up depolymerization: 1.0 g of Nylon-6 in a 100 mL Schlenk flask.

flsolated yield after recrystallization of the product; see supplemental information for details.





To examine the scalability of this reaction, the 3-mediated Nylon depolymerization was carried out on a 1-g scale using a 0.2 mol % catalyst loading. A NMR yield of 97% (94% isolated yield) was obtained (Table 1, entry 8).

Another consideration is the depolymerization temperature. Commodity polymer chemical recycling typically utilizes energy-intensive high temperatures with competing thermal decomposition.<sup>2,40</sup> Although the present 240°C temperature is lower than those typically used in Nylon depolymerizations (>300°C), <sup>25,27,36,41</sup> it is above the 218.3°C Nylon-6 melting point. 14 Thus, catalytic studies were next conducted at 220°C with 0.2-1.0 mol % Cp\*2LaCH(TMS)2 (3) and provided up to 95% yields (Table 1, entries 9 and 10). To probe  $Ln^{3+}$  size effects, catalysts  $Ln^{3+} = Lu^{3+}$ (4, i.r. = 0.97 Å) and psuedo-lanthanide  $Y^{3+}$  (5, i.r. = 1.01 Å) were compared with La catalyst 3 (i.r. = 1.17 Å). Under identical solventless reaction conditions (Table 1, entries 9-13), the performance of the Lu (4) and Y (5) analogs to 3 is significantly inferior. Regarding structural effects, note that lanthanocene catalyst 3 is 238× more active than catalyst 1 at 220°C (0.5 vs. 118.8 (mol  $\varepsilon$ -caprolactam)·(mol La)<sup>-1</sup>·(h)<sup>-1</sup>), highlighting the advance afforded by metallocene ligation. Interestingly, these rates qualitatively parallel activity trends in Cp\*2Ln-catalyzed olefin hydroelementation and other additions to C=C/C≡C unsaturations.<sup>29,30</sup> These reflect a mix of electronic and steric effects, with the latter predominant, reflecting crowding in the insertive C-C unsaturation transition state. 30,42

Note that smaller i.r. Y<sup>3+</sup> metallocenes are known to display high thermal stabilities, likely reflecting lower reactivities in undesired intramolecular thermolytic pathways. <sup>29,43,44</sup> Note also that Y lies at a lower production energy cost<sup>45</sup> and environmental impact metric. <sup>35,46</sup> With these attractive Y features, we sought ligand modification beyond poorly active Y<sup>NTMS36</sup> and promising Cp\*<sub>2</sub>YCH(TMS)<sub>2</sub> (5).

Ansa-lanthanocenes, Me<sub>2</sub>SiCp"<sub>2</sub>LnR (Cp" =  $\eta^5$ -Me<sub>4</sub>C<sub>5</sub>) with chelating ancillary  $\pi$ -ligands and larger "bite" angles (Figure 2B; 2) display substantially enhanced catalytic activities in unsaturated C-C insertions into Ln–N bonds (10–100× increased TOFs) vs. their Cp\*2LaR analogs. 38,47,48 Additionally, the chelating ansa ligation may further enhance the thermal stability of Y catalytic systems.<sup>49</sup> Thus, the complex Me<sub>2</sub>SiCp"<sub>2</sub>YCH(TMS)<sub>2</sub> (6) was prepared and first examined for virgin Nylon-6 powder depolymerization. 38,50 Remarkably, chelation of the Y coordination sphere dramatically increases the depolymerization yield from 2% to 94% ( $Cp_2^*Y- \rightarrow$ Me<sub>2</sub>SiCp"<sub>2</sub>Y-; 43 × increased rate) under identical reaction conditions (Table 1, entry 13 vs. 15), illustrating the effects of this ancillary ligand "engineering." Further extending the reaction time to 2 h effects a >99% conversion of Nylon-6 by catalyst 6 (Table 1, entry 16). This ligand manipulation essentially imbues a more desirable Y center with La center catalytic properties. This is also supported by steric effect free-volume contours ( $%V_{free}$ )<sup>51</sup> computed (Figure 3) for catalysts 3, 5, and 6 from DFT-optimized structures (vide infra), which track the respective experimental catalytic activity trends discussed above.

#### Post-consumer Nylon depolymerization

Encouraged by the high activities of catalysts 3 and 6 for pristine Nylon-6, the depolymerization of post-consumer products was next examined (Table 2). Samples were finely chopped, dried, and subjected to depolymerization trials (see supplemental information for details). Note that potassium hydroxide (KOH) treatments were applied only to powdered Nylon-6 samples to neutralize carboxylic end-groups for kinetic studies (vide infra) but not to post-consumer products due to the large Nylon particle sizes. Regarding ocean pollution, a 2-year-old discarded fishing net



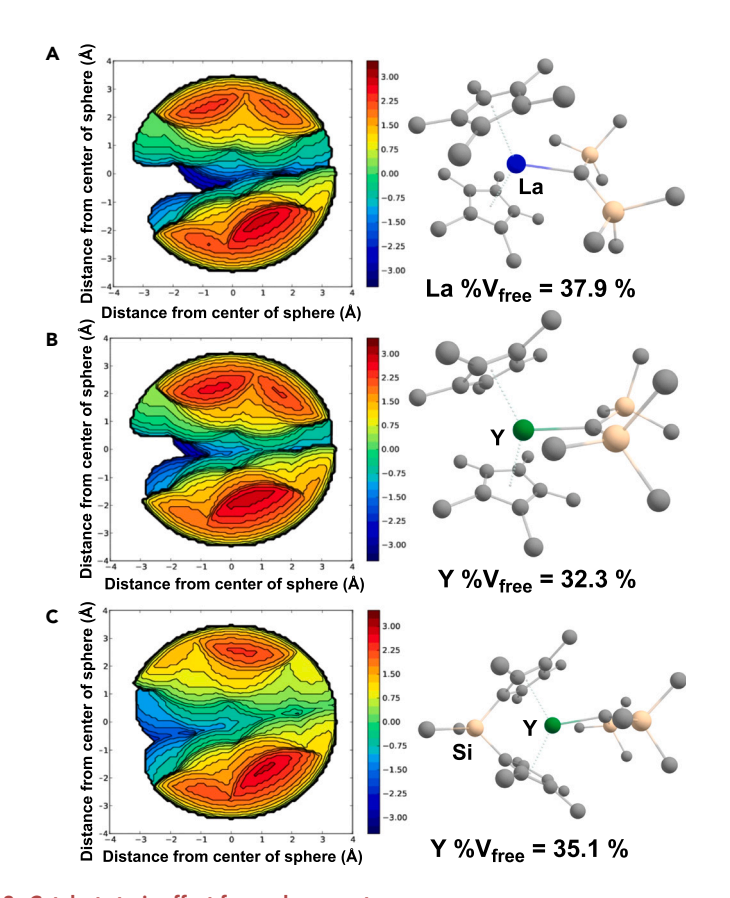


Figure 3. Catalyst steric effect free volume contours Computed percent free volume ( $%V_{free}$ ) contours based on DFT-optimized structures for (A)  ${\sf Cp*_2LaCH(TMS)_2}\ \textbf{(3)};\ (B)\ {\sf Cp*_2YCH(TMS)_2}\ \textbf{(5)};\ {\sf and}\ (C)\ {\sf Me_2SiCp''}_2{\sf YCH(TMS)_2}\ \textbf{(6)}.$ 

was first tested. Catalyst 1 rapidly sublimes from the catalyst + finely chopped mixture, yielding minimal  $\epsilon$ -caprolactam (<1% yield; Table 2, entry 1) after 24 h/240°C. Note that catalyst 1 provides moderate depolymerization yield (78%) for one case of consumer Nylon-6 only when special pretreatment is applied

Table 2. Catalytic depolymerization of post-consumer Nylon plastics										
Entry	Nylon plastic	Catalyst	Catalyst loading (mol %) <sup>a</sup>	Time (h)	Yield (%) <sup>b</sup>	TOF°				
1	fishing net	1	5.0	24	<1	<0.1				
2	fishing net	3	5.0	24	65	0.542				
3	fishing net	5	5.0	24	95	0.792				
4	fishing net	6	1.0	6.0	94	15.7				
5	carpet fiber	6	1.0	6.0	>99	16.7				
6	Nylon yarn	6	1.0	6.0	87	14.5				

<sup>1.0</sup> amol % loadings are calculated assuming 100% of Nylon-6 in these post-consumer products, except for entry 8 (see footnote<sup>d</sup>).

1.0

1.0

6.0

12

12

99

89ª

16.5

7.41

7.92

t-shirt

medical gloves<sup>d</sup>

fishing net + water bottle cap 6

<sup>&</sup>lt;sup>b</sup>Yields determined by <sup>1</sup>H NMR with a mesitylene internal standard.

<sup>&</sup>lt;sup>c</sup>Turnover frequencies (TOFs) calculated in units of (mol  $\epsilon$ -caprolactam)·(mol Cat.)<sup>-1</sup>·(h)<sup>-1</sup>.

 $<sup>^{\</sup>rm d}$ 355 mg sample of medical gloves, which contain 100 mg Nylon-6 (31%).

<sup>&</sup>lt;sup>e</sup>Determined from Nylon-6 content in medical glove sample; see supplemental information for details. <sup>f</sup>Fishing net: water bottle cap in a 1:1 mass ratio.





(cryogenically milled Nylon yarn). <sup>36</sup> For catalyst 3, the modest yield at high loadings (Table 2, entry 2) likely reflects poor mixing and catalyst thermal instability, whereas thermally more robust Y catalyst 5 delivers higher yields (Table 2, entry 3), and ansametallocene Y catalyst 6 achieves a remarkable 94% yield in only 6 h (Table 2, entry 4), paralleling the results with powdered Nylon-6 (vide supra), arguably reflecting enhanced activity and stability. In sum, ansa-yttrocene 6 is  $\sim$ 29 x more effective in fishing net recycling than metallocene La catalyst 3, favoring dominant ancillary ligation vs. metal i.r. effects.

To probe the scope of 6-catalyzed depolymerization, other post-consumer Nylons were next surveyed. Carpet waste has a global environmental impact<sup>52</sup> with an annual production of 12 billion ft<sup>2</sup> only 5% of which is recycled and 91% is landfilled. In the US, 4 billion lb of carpet is landfilled annually, <sup>19,53</sup> and with ~75% of carpets composed of Nylon, <sup>52,53</sup> recycling ε-caprolactam from carpet waste is attractive. Pleasingly, the carpet fiber was fully depolymerized with 1 mol % of 6, yielding ε-caprolactam quantitatively (Table 2, entry 5). Under the same conditions, post-consumer Nylon-6 yarn afforded ε-caprolactam in 87% yield (Table 2, entry 6). Nylon fabrics, known for durability and water resistance, are utilized in shirts, swimsuits, footwear, etc. A Nylon t-shirt was next subjected to depolymerization using catalyst 6, producing ε-caprolactam in 99% yield (Table 2, entry 7).

To further define the depolymerization scope, we turned to waste plastics from the COVID-19 pandemic-associated demand for gloves and face masks.<sup>54</sup> Medical gloves containing Nylon-6 were finely chopped and exposed to catalyst 6 (Table 2, entry 8), affording an 89% yield with respect to the Nylon content of  $\varepsilon$ -caprolactam (see supplemental information details). Note that commodity Nylons such as carpet waste, t-shirts, and medical gloves all contain varying amounts of diverse chemical additives such as dyes, stabilizers, and lubricants, 55 yet the performance of catalyst 6 remains essentially unchanged. Finally, in real-world marine plastic wastes, fishing net debris is typically mixed with other plastics, such as containers, bags, straws, bottle caps, etc. Besides Nylon-6, polyolefins, such as polyethylene and polypropylene (PE and PP), are most common in ocean plastics. <sup>12</sup> To assess the applicability of catalyst 6 to post-consumer plastic mixtures, the depolymerization of end-of-life Nylon-6 fishing nets was next investigated for a sample admixed with PE water bottle caps in a 1:1 mass ratio. This afforded ε-caprolactam in 95% yield (Table 2, entry 9), whereas the inert PE was recovered unchanged, as evidenced by <sup>1</sup>H NMR (Figure S26). Thus, 6 is compatible with mixed Nylon-6-polyolefin mixed wastes and can be used to separate end-of-life Nylon-6 from mixed plastic, yielding the valuable caprolactam monomer. Note that catalyst 6 is highly robust at 1 mol % loading to depolymerize a broad scope of Nylon-6 samples, including a variety of pre- and post-consumer articles without any special pretreatment, in marked contrast to homoleptic catalyst 1 that is only applicable to KOH-treated and finely ground Nylon-6 samples.

#### Circularity for end-of-life fishing net

To "close the loop" for a fully circular end-of-life Nylon economy, it was of interest to determine if the recovered  $\epsilon$ -caprolactam could be re-polymerized to yield high-quality Nylon-6. Thus,  $\epsilon$ -caprolactam recovered from the large-scale depolymerization of end-of-life fishing net was re-polymerized using an anionic polymerization procedure<sup>54</sup> with NaH and N-acetylcaprolactam activators at 140°C. NMR, matrix-assisted laser desorption ionization-time-of-flight mass spectrometry (MALDI-TOF MS), and gel-permeation chromatography (GPC) analyses were used to confirm the repurposed Nylon-6 identity and purity (Figures S41–S52). Impressively, the recycled polymer obtained in 99.3% yield with  $M_n=43.6$  kg mol $^{-1}$  and  $^{1}H$  NMR in



500 MHz).

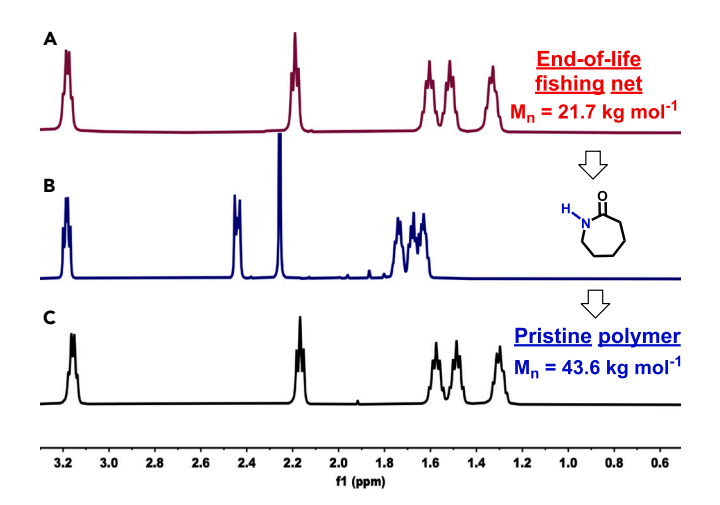


Figure 4. Collected NMR spectra for depolymerization-repolymerization experiments  $^1$ H NMR spectra of (A) an end-of-life fishing net (drops of CDCl $_3$  + TFE, 500 MHz); (B) crude  $\epsilon$ -caprolactam product collected from depolymerization of the fishing net (CDCl $_3$ , 500 MHz); and (C) repurposed Nylon-6 obtained from the subsequent re-polymerization (drops of CDCl $_3$  + TFE,

Figure 4, is of comparable or superior quality compared with the original fishing net waste ( $M_n = 21.7 \text{ kg mol}^{-1}$ ). This methodology highlights the attraction of Nylon chemical recycling by an efficient monomer recovery process and effectively closes the loop for end-of-life Nylon plastic, imbuing new value to the abandoned fishing net.

#### Mechanistic analysis of Nylon-6 depolymerization

#### Productivity of catalyst 1 vs. catalyst 3

Catalyst 3 was selected to probe the metallocene-mediated depolymerization mechanism because it enables a more realistic comparison with homoleptic catalyst 1 bearing the same La<sup>3+</sup> center. Note that for the virgin Nylon-6 sample, the average number of monomer units in a polymer chain (i.e., degree of polymerization, DP) is estimated to be  $\sim$ 130 from M<sub>n</sub> = 14,800 g mol<sup>-1</sup>. For a 1 mol % catalyst loading, the estimated polymer chain: La<sup>3+</sup> ratio is  $\approx$  1:1.3, indicating slightly more than 1 La<sup>3+</sup> catalyst molecule per one polymer chain is available, and in principle, assuming the depolymerization process involves stepwise excision of caprolactam units as the catalyst 3 moves along the chain, no interchain La<sup>3+</sup> "hopping" is required to consume one Nylon-6 chain. This agrees with the experimental data (Table 1, entries 1 and 4) that both catalysts 1 and 3 provide reasonable activities and yields at 1 mol % catalyst loading (69% and 91%, respectively). However, for a lower catalyst loading of 0.2 mol %, the calculated polymer chain: La<sup>3+</sup> ratio is  $\approx$  5:1, and in this scenario, the La<sup>3+</sup> catalyst must "hop" between polymer chains to achieve high depolymerization conversions. Under these conditions, catalyst 1 only provides a 5.6% ε-caprolactam yield (Table 1, entry 2), whereas catalyst 3 is barely impacted by the lower loading (Table 1, entries 6-8, 11).

To gain further insight into the superior performance of catalyst 3, further experiments were carried out. It was previously shown that in Nylon-6 depolymerization by catalyst 1, nearly all three  $TMS_2N$ -ligands participate—2.5 equiv of  $TMS_2NH$  are released in the reaction onset. It therefore seems unlikely that catalyst 1 can readily interchain hop following the consumption of a single Nylon chain, reflecting the aforementioned  $La^{3+}$ -polymer "cross-linking" and poor tris-amido active site





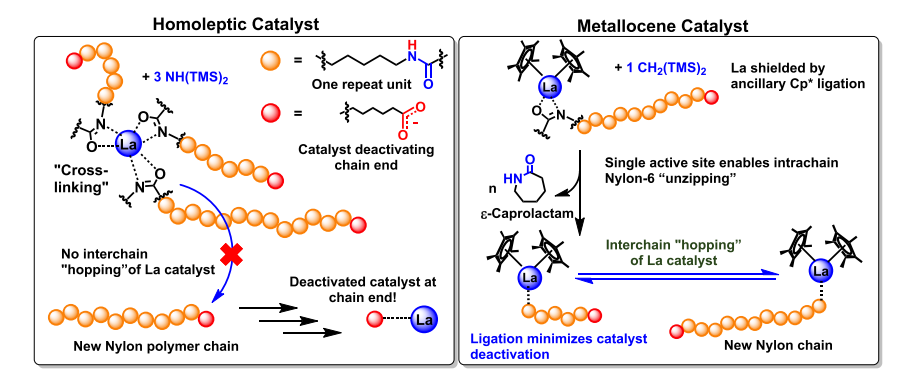


Figure 5. Illustration of different depolymerization pathways for homoleptic catalyst 1 (left) and metallocene catalyst 3 (right).

stereocontrol (Figure 5, left). Instead, catalyst deactivation by a Nylon chain-end carboxylate/carboxylic acid is plausible (see below for details). In contrast, the non-dissociable Cp\*<sub>2</sub> ligands of catalyst 3 can sterically shield the La center and plausibly hinder the undesired catalyst cross-linking/immobilization. This may enable catalyst 3 interchain-hopping at low catalyst loadings, which is supported by DFT analysis (vide infra).

To probe these mechanistic aspects further, *in situ* <sup>1</sup>H NMR spectra at the onset of depolymerization were acquired (see supplemental information section kinetic studies). The data reveal gradual protonolysis of the La-CH(TMS)<sub>2</sub> linkage with ~95% of the expected CH<sub>2</sub>(TMS)<sub>2</sub> obtained. Concurrently, only trace amounts (<5% yield) of a Cp\*H product are detected in accordance with the stability of the Ln-Cp\* ligation.<sup>29,30</sup> Here, we propose a plausible process for Nylon-6 recycling via intrachain "unzipping" by catalyst 3 (Figure 5, right). Unlike catalyst 1, the deactivation of catalyst 3 at the chain ends can be minimized by effective interchain hopping, achieving high-yield depolymerization at low catalyst loadings.

#### Chain-end catalyst deactivation and kinetic analysis

Next, catalyst deactivation at the polymer chain ends was investigated. After reaching full depolymerization conversions, the catalytic species is likely to reach carboxylate groups, forming an inert carboxylate complex—Figure 6 shows a plausible structure. By this hypothesis, following the consumption of an initial polymer batch,

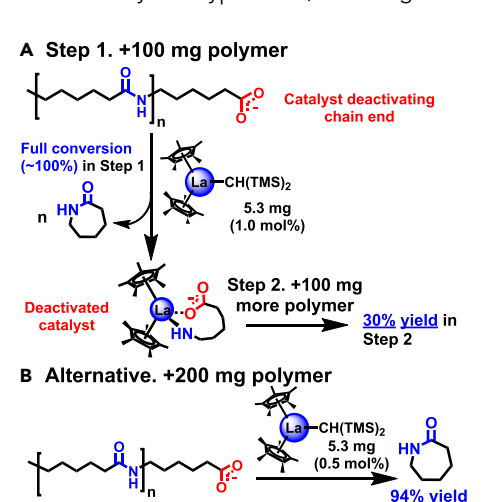
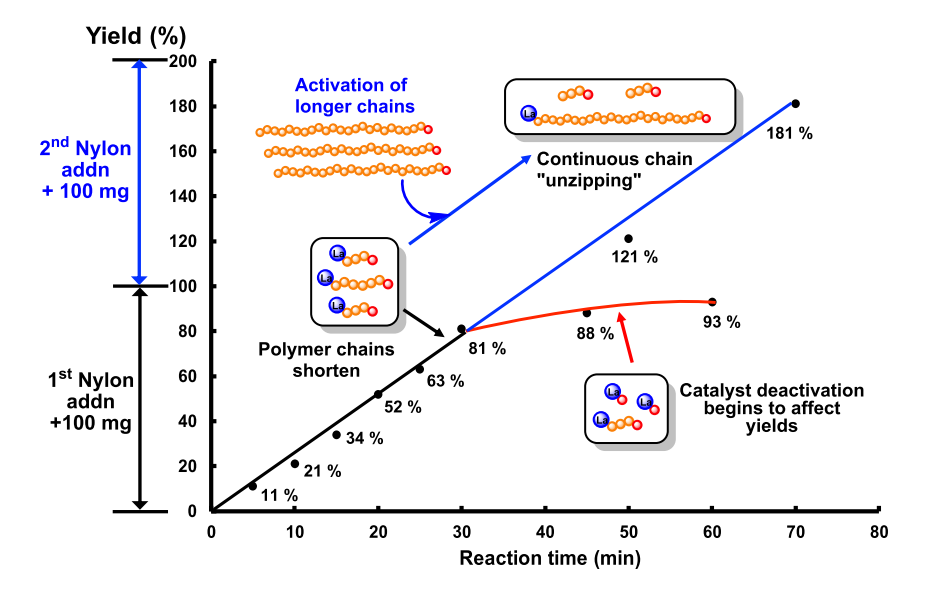


Figure 6. Experiments to define catalyst deactivation by Nylon-6 chain ends
See section catalyst reusability test and continuous depolymerization experiments of the supplemental information for experimental details.





**Figure 7. Kinetic study to characterize Nylon-6 depolymerization pathway**Reaction conditions 0.2 mol % of catalyst **3**, 240°C, 100 mg Nylon-6. Yields calculated for 1<sup>st</sup> polymer addition. Black and red traces show the kinetic profile of 1<sup>st</sup> polymer addition. Blue line represents continuous linear yield growth on 2<sup>nd</sup> polymer addition at 30 min.

the residual reaction mixture should exhibit far lower activity when exposed to a second 100 mg Nylon addition. Under the catalytic conditions employed in Table 1, entry 5, the depolymerization rate for the second 100 mg is significantly lower, with a 30% yield (Figure 6A). In contrast, depolymerization of a combined 200 mg polymer sample, added in a non-stepwise manner, under the same catalytic conditions, achieves a 94% yield (Figure 6B).

In Figure 7, the kinetic profile/ε-caprolactam yield of 3-mediated depolymerization is plotted vs. the reaction time with a low catalyst loading (0.2 mol %). A linear increase in ε-caprolactam yield is evident over the first 30 min (up to 81% yield; Figure 7, black line), followed by saturation in the later stages (30-60 min) of reaction (Figure 7, red curve). Because catalyst deactivation most likely occurs at the carboxvlate chain ends, this suggests that the declining reaction rate after 30 min occurs as the depolymerization of shorter chains is completed. To test this hypothesis, two depolymerization reactions were carried out under identical conditions and halted at 30 min to avoid reaching full conversion and catalyst deactivation. To these reaction residues, the same amounts of pristine Nylon-6 were added without quenching any reaction intermediates, and the mixtures were allowed to react for another 20 and 40 min, respectively (see supplemental information for experimental details). The results demonstrate a continuous linear growth of  $\varepsilon$ -caprolactam yield (Figure 7, blue line) without saturation after 30 min, in contrast to the initial kinetic trend (red curve). In this case, adding long polymer chains at 30 min allows the La to hop from the shorter chains to longer chains so that a decrease of the catalyst loading of 3 from 0.2 to 0.1 mol % occurs in the addition of new polymer chains before reaching full depolymerization conversion.

#### Catalyst durability and continuous depolymerization process simulation

The present model studies suggest the potential for Nylon-6 depolymerization with ultra-low catalyst loadings in a continuous rather than batch process. As a demonstration of this concept, the experiments presented above involved a catalyst loading reduction with catalyst 3 to 0.2 to 0.1 mol % on addition of fresh Nylon-6





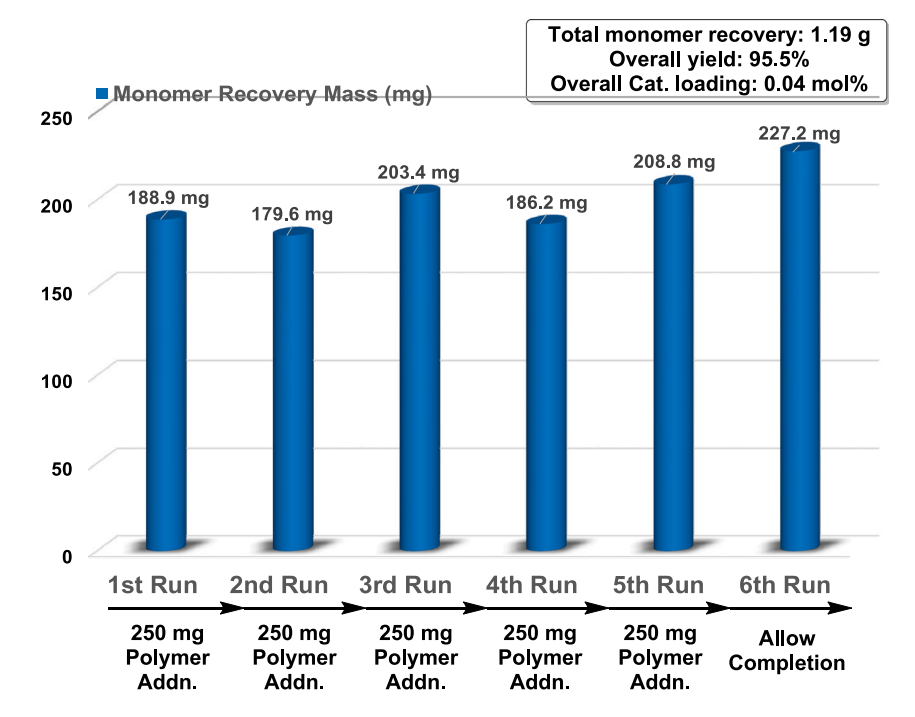


Figure 8. Catalyst recyclability test for multi-batch continuous depolymerization simulation Reaction conditions: 2.7 mg of catalyst 3 (0.0018 mmol), overall of 0.04 mol % loading,  $240^{\circ}\text{C}$ ,  $5 \times 250 \text{ mg}$  Nylon-6 additions. Reaction times: 1.5 h for run 1; 2 h for run 2–5; and overnight for run 6. See supplemental information for details.

before reaching full conversion of the first batch (Figure 7). To further probe the recyclability of the present metallocene catalysts, a multi-batch simulated continuous depolymerization experiment was performed in a larger-scale reactor with a 0.04 mol % loading of catalyst 3 (Figure 8; see supplemental information for experimental details). Before each run (runs 2–5), the caprolactam collected from the previous run was removed, weighed, and 250 mg of fresh Nylon-6 was added to the reactor containing the same catalyst 3 charge. The results show steady caprolactam yields across all catalyst recycling experiments, indicating that catalyst 3 retains a high level of activity through each run. The final (6<sup>th</sup>) run was performed without fresh Nylon addition to allow full completion of the depolymerization process, providing an overall Nylon-6 yield of 95.5% using an ultra-low overall catalyst loading of 0.04 mol %.

#### DFT analysis (see computational details in supplemental information)

A detailed Gibbs free energy profile was computed by DFT for catalyst 3 (Figure 9) to connect with the experimental mechanistic data. Note that the earlier DFT analysis of the homoleptic catalysts was limited by the complexity of the three Nylonic ligands, and a simple, informative model for Nylon recycling could not be generated. In this study, DFT calculations were performed on a realistic Nylon-6 dimer model to accurately simulate the coordination of the well-defined metallocene catalysts to an actual polymer. The initial step involves intramolecular Cp\* ligand C-H activation to quantitatively eliminate CH<sub>2</sub>(TMS)<sub>2</sub> (validated by  $^1$ H NMR) and form a lanthanocene "tuck-in" complex  $^{56}$  (INT2). Note that this computed pre-catalyst thermolytic process is in good agreement with previous results from this laboratory.  $^{34}$  This step is slightly exergonic ( $\Delta G = -3.6$  kcal mol $^{-1}$ ) with a barrier of  $\Delta G^{\ddagger} = 29.2$  kcal mol $^{-1}$  (TS1), hence relatively rapid on the catalytic timescale (see Figure S56 for detail). By contrast, this activation step for catalyst 2 with a less reactive ligand (–NTMS) is



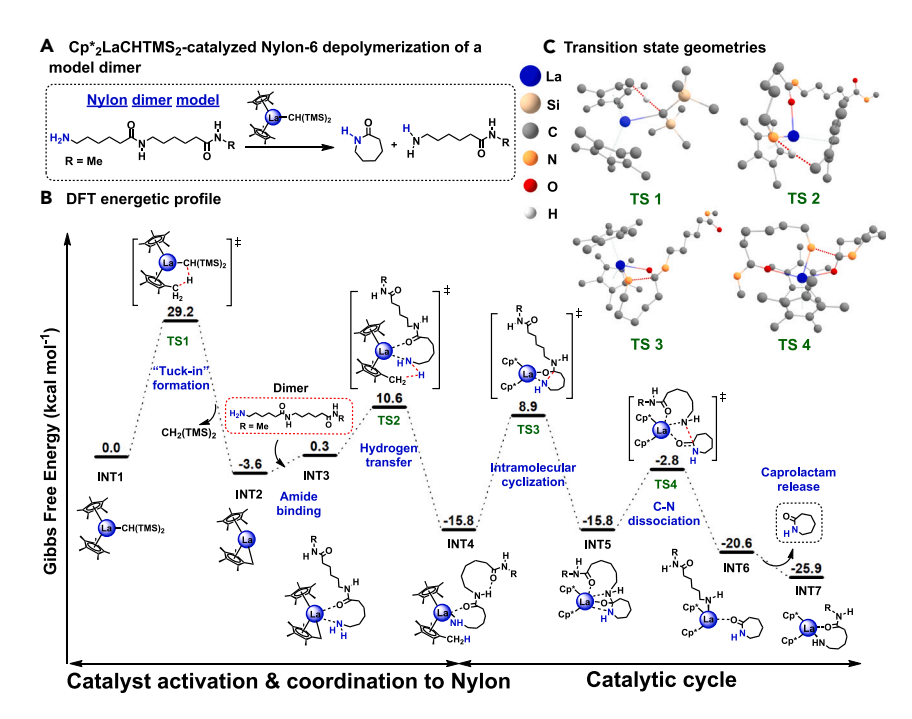


Figure 9. DFT analysis of Nylon-6 depolymerization using a model dimer

Gibbs free-energy profile in solution phase (kcal  $mol^{-1}$ ).

- (A) Computed Nylon dimer model reaction.
- (B) DFT-derived energetics.
- (C) Computed transition state geometries. Reaction pathways are highlighted in dashed lines. H atoms not involved in reactions are deleted for clarity.

calculated to be unfavorable ( $\Delta G = 19.2 \text{ kcal mol}^{-1}$ ) with a far higher barrier ( $\Delta G^{\ddagger} = 39.5 \text{ kcal mol}^{-1}$ ) to yield INT2, in accord with its low activity (Figure S57). Next, coordination of the La center to the amide carbonyl group is slightly endergonic ( $\Delta G = 3.9 \text{ kcal mol}^{-1}$ ), yielding INT3, which is stabilized by intramolecular chelation by the polymer –NH<sub>2</sub> chain end. Next, the tuck-in moiety reverts to the Cp\*<sub>2</sub>La metallocene in an exergonic H<sup>+</sup>-transfer from the terminal amine ( $\Delta G = -16.1 \text{ kcal mol}^{-1}$ ; barrier  $\Delta G^{\ddagger} = 10.3 \text{ kcal mol}^{-1}$ ) to yield INT4. This step is supported by a Cp\*<sub>2</sub>Ln-catalyzed hydroamination study in which rapid protonolysis of INT2 by amine substrates was observed experimentally.<sup>34</sup> Once INT4 enters the catalytic cycle (Figure 10),

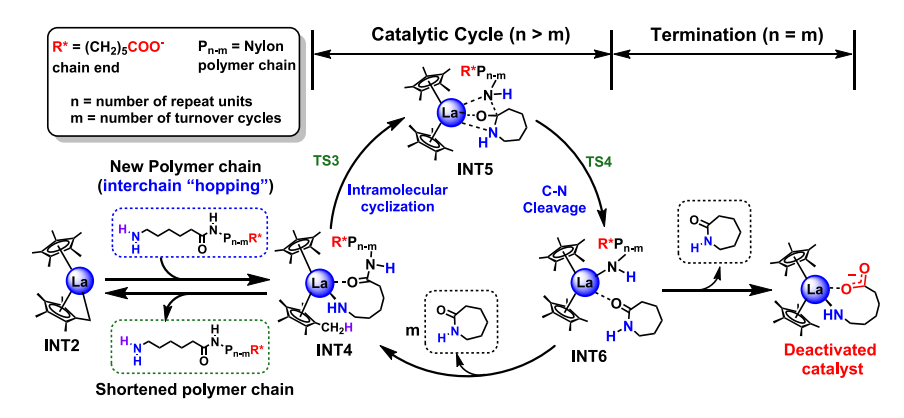


Figure 10. Proposed catalytic cycle for the catalytic depolymerization of Nylon-6

Schematics of the interchain hopping and end-chain catalytic deactivation mechanisms are included. A counter cation is not included in the deactivated catalyst structure for clarity of viewing.





an intramolecular cyclization yields INT5 in a thermoneutral step ( $\Delta G = 0.01$  kcal mol<sup>-1</sup>) with a barrier of  $\Delta G^{\ddagger} = 24.6$  kcal mol<sup>-1</sup> (TS3), which is the rate-determining step in the cycle. The importance of utilizing a dimer model is highlighted by mimicking a polymer chain to provide additional coordination by an adjacent amide, which stabilizes INT5 by 7.2 kcal mol<sup>-1</sup> (Figure S58) and more realistically depicts a La-polymer binding scenario. Moreover, the barrier for the less active Y analog (catalyst 5) of this rate-determining step (TS3) is computed to be 1.9 kcal mol<sup>-1</sup> higher than for catalyst 3 (Figure S59), in agreement with experimental results (Table 1). Next, INT6 is formed via an exergonic ( $\Delta G = -4.8$  kcal mol<sup>-1</sup>) C-N dissociation step, which has a barrier of  $\Delta G^{\ddagger}_{\ddagger} = 10.8$  kcal mol<sup>-1</sup> (TS4). Lastly,  $\varepsilon$ -caprolactam is released in a slightly exergonic step ( $\Delta G = -5.4$  kcal mol<sup>-1</sup>), yielding INT7 with a second Nylon-6 monomer coordinated to the La center to complete the catalytic cycle (also see Figure 10).

Next, the interchain hopping mechanism was investigated to support the 3-mediated depolymerization pathway proposed in Figure 5. Besides continuing the catalytic cycle with the coordinated polymer chain, another possible pathway for INT4 is to undergo a polymer-polymer exchange via INT2 in reversible steps (Figure 9). To evaluate this pathway, a concentration modeling was performed by computing the interchain hopping of catalyst 3 between two Nylon dimers (Figure S60). The simulation shows that the La<sup>3+</sup> center hops within seconds at 240°C, and equilibration between Nylon chains (meaning rapid Nylon chain interchange) occurs within 3 minutes. Chain-end catalyst deactivation (Figure 10, n = m) was also examined computationally (Figure S61). In a computed structure for the deactivated catalyst, La<sup>3+</sup> is coordinated to the carboxylate chain end and a terminal primary amine. This complex is found to be unfavorable ( $\Delta G$  = 1.7 kcal mol<sup>-1</sup>) for hopping to a new polymer chain (simulated by a dimer model) and regenerating the active species INT4, which validates this deactivation mode, in good agreement with experiment under the present reaction conditions (Figure 6).

#### **Conclusions**

This study demonstrates rational catalyst ligand design as a promising pathway to realize rapid, selective, and solventless Nylon-6 plastic chemical recycling. A series of earth-abundant lanthanide and yttrium metallocene and ansa-metallocene catalysts exhibit far higher activity and durability than homoleptic tris-amido lanthanide catalysts. For example, catalyst 3 is a highly effective catalyst for the depolymerization of powdered Nylon-6, affording up to >99% yield of ε-caprolactam) at temperatures as low as 220°C and catalyst loadings as low as 0.2 mol %. This catalyst can be reused multiple times without deactivation in a simulated continuous mode to achieve an ultra-low catalyst loading of 0.04 mol %. These conditions, to the best of our knowledge, are the mildest to date for Nylon-6 depolymerization in the peer-reviewed literature. Experimental and DFT mechanistic analyses reveal effective depolymerization pathways involving catalytic intrachain unzipping assisted by the catalyst  $\pi$ -ancillary ligand steric constraints, as well as interchain hopping and chain-end catalyst deactivation mechanisms. For the more challenging waste Nylon-6 commodity products, ansa-yttrocene complex 6 exhibits a far higher activity and thermal stability than lanthanocene 3 and efficiently depolymerizes a variety of end-of-life Nylon plastics, including fishing nets, carpets, clothing, gloves, as well as a mixed PE + Nylon-6 mixture. Furthermore, a "closed-loop" recycling model is demonstrated by re-polymerizing waste fishing net-derived  $\epsilon$ -caprolactam (Figure 4) to high-quality Nylon-6 of higher M<sub>n</sub> than the original fishing net.





#### **EXPERIMENTAL PROCEDURES**

#### Resource availability

#### Lead contact

Further information and requests for resources should be directed to and will be fulfilled by the lead contact, Prof. Tobin J. Marks (t-marks@northwestern.edu).

#### Materials availability

Materials will be made available from the lead contact after the execution of a material transfer agreement.

#### Data and code availability

All data needed to support the conclusions of this manuscript are included in the main text and/or the supplemental information.

#### Materials and methods

Catalyst 1 was obtained from Strem Chemicals. Cp\*2LaN(TMS)2 (2), Cp\*2LaCH(TMS)2 (3),  $Cp_2LuCH(TMS)_2$  (4),  $Cp_2YCH(TMS)_2$  (5), and  $Me_2SiCp_2YCH(TMS)_2$  (6) were synthesized according to published reports. <sup>37–39</sup> Catalyst loadings are calculated with respect to the repeat unit molar mass of Nylon-6. All polymers were washed with 1 M KOH solution overnight, <sup>36</sup> filtered, washed with deionized H<sub>2</sub>O, and dried under a high vacuum at 100°C for at least 24 h prior to use. Pristine Nylon-6 powder with a mean particle size of  $15-20 \mu m$  and a molecular mass ( $M_p$ ) of 14,800 g/mol (as determined by GPC) was obtained from Goodfellow. All manipulations in catalyst synthesis were carried out with the exclusion of O<sub>2</sub> and moisture in oven-dried Schlenk-type glassware on either a dual-manifold Schlenk line, interfaced to a high-vacuum manifold (10<sup>-6</sup> Torr), or in an Argon-filled MBraun glovebox with a high-capacity recirculatory (<1 ppm O<sub>2</sub>). All depolymerization reactions were assembled by mixing the polymer and the appropriate catalyst in an Argon-filled MBraun glovebox in cylindrical 50 mL Schlenk tubes. Heating was supplied by a customized aluminum heating block with a fitted hole for the Schlenk tubes. See Figure S1 for a typical depolymerization setup.

#### Physical and analytical methods

NMR spectra were recorded on a Varian Bruker Advance III HD system equipped with a TXO Prodigy probe (500 MHz) spectrometer. Chemical shifts ( $\delta$ ) for <sup>1</sup>H NMR are referenced to the internal solvent. NMR spectra of re-polymerized Nylon-6 were measured by dissolving the polymer samples in trifluoroethanol (TFE) and a few drops of CDCl<sub>3</sub>. Mass Spectral data were collected on Bruker Rapiflex MALDI-TOF using FlexControl data acquisition software and processed using FlexAnalysis software for data analysis. Polymer samples for MALDI-TOF analyses were dissolved in hexafluoroisopropanol (HFIP) at a 5 mg/mL concentration. The matrix used was 2-(4-hydroxyphenylazo)-benzoic acid (HABA). The layered sample preparation technique was used in which 2 μL of saturated HABA matrix in HFIP solution was applied to the sample target, dried in air, covered with a  $2-\mu L$  layer of sample solution, dried in air, and followed by a final layer of matrix solution. GPC was used to analyze the number average molecular weight  $(M_n)$ , weight average molecular weight  $(M_w)$ , and molecular weight dispersity indices (Đ) of Nylon-6 samples. An Agilent Infinity II 1260 high-performance liquid chromatography (HPLC) system was coupled with Wyatt MiniDAWN TREOS multi-angle light scattering (MALS, 3 angles) and Optilab T-rex differential refractive index (RI, 658 nm) detectors. Polymer concentrations of  $5.0 \pm 0.05$  mg/mL in HFIP (ChemImpex) amended with 20 mM sodium trifluoroacetate (NaTFAc, Sigma-Aldrich) were prepared by dissolving each polymer at room temperature on a shaker plate, followed by filtration through a 0.2 µm syringe filter.





Samples were injected at a volume of 100  $\mu$ L into the system at a flow rate of 0.35 mL/min (HFIP with 20 mM NaTFAc) through 3 Plgel-HFIP columns in series with a guard column at 40°C. Astra 7 software was used to determine absolute  $M_{\rm n}$ ,  $M_{\rm w}$ , and dispersity ( $D_{\rm n}$ ,  $M_{\rm w}/M_{\rm n}$ ) using dn/dc values calculated by assuming 100% mass recovery using the known concentration of each sample. Polymethyl methacrylate and PE terephthalate standards were used to check instrumentation and validate results.

#### General procedures for depolymerization reactions

In a glove box, a 50 mL oven-dried Schlenk tube was charged with a magnetic stir bar, pristine Nylon-6 fine powder (or post-consumer Nylon product), and finely ground catalyst. The vessel was sealed tightly, and the polymer and catalyst were thoroughly mixed by stirring at room temperature for approximately 5 min. The Schlenk tube was then evacuated to  $10^{-3}$  Torr, sealed, and heated to the specified temperature with slow magnetic stirring (50–100 rpm) for the specified time. Reaction time was recorded starting 2.5 min after the reaction tube was placed in the heating block because it requires an average of 2.5 min for the reaction to reach the depolymerization temperature and the polymer to begin melting. During the reaction, the  $\varepsilon$ -caprolactam product sublimes from the hot reaction zone and deposits as a crystalline layer on the cold wall of the reactor. After cooling to room temperature, the soluble part of the reaction mixture was dissolved in 3–4 mL of deuterated solvent, and mesitylene was added as an internal standard. A sample of this solution was withdrawn for NMR analysis. Yields were quantified by  $^1$ H NMR, comparing the signal integrals of  $\varepsilon$ -caprolactam and mesitylene.

#### Computational details

All quantum chemical calculations were performed using the ORCA 5.0.3 package. 57,58 The geometric optimizations were calculated with the hybrid functional of PBE0<sup>59,60</sup> with the def2-SVP basis set of the Ahlrichs group 61,62 along with dispersion corrections quantified by the DFT-D3<sup>63</sup> method with Grimme's Becke-Johnson (BJ) damping.<sup>64</sup> Frequency calculations were performed at the same level of theory, and all minima were confirmed to have zero imaginary frequency modes, whereas transition states showed exactly one negative frequency mode. The single-point calculations were performed at a higher level of theory, PBE0-D3/def2-TZVP, using the solvation model based on density (SMD).<sup>65</sup> N-methylformamide was chosen as the solvent because it represents the solvent environment of the melted Nylon-6 polymer. In addition, to accelerate the DFT calculations, resolution of identity approximation (RI)<sup>66</sup> was used for the Coulomb integrals and efficiently computed the exchange terms using the "chain-of-spheres" (COSX)<sup>67</sup> approximation with the def2/J auxiliary basis set. The visualization software used was Chemcraft. 68 Three different configurations for the coordination of Nylon-6 dimer model to catalysts were considered, namely, "linear," "crest" (conformer searched using the CREST package<sup>69</sup>), and "curve." See details in the supplemental information. Shermo<sup>70</sup> was used for the Gibbs free energy files based on the frequency and single-point energy calculations with Grimme's entropy interpolation<sup>71</sup> for quasi rigid-rotor harmonic oscillator (QRRHO) approximation. All thermodynamic values are reported at 1 atm and at 240°C with a concentration of 1 M to capture the variation of Gibbs free energy due to concentration change from the gas phase (1 atm) to the liquid phase standard state (1 M). Concentration modeling was performed by Concvar<sup>72</sup> based on the calculated Gibbs free energy profile.

#### SUPPLEMENTAL INFORMATION

Supplemental information can be found online at https://doi.org/10.1016/j.chempr. 2023.10.022.

Chem Article



#### **ACKNOWLEDGMENTS**

The support of RePLACE (Redesigning Polymers to Leverage A Circular Economy), funded by the Office of Science of the U.S. Department of Energy via award no. DE-SC0022290 (T.J.M., L.Y., K.B., L.J.B., and X.L.), is gratefully acknowledged. Y.K. acknowledges support from the Office of Basic Energy Sciences, US Department of Energy (DE-FG02-03ER15457) to the Institute for Catalysis in Energy Processes (ICEP) at Northwestern U. J.O.R. acknowledges support from NSF CAT Program grant CHE-1856619. This work made use of the IMSERC NMR facility at Northwestern U., supported by NSF (CHE-1048773). This work used Expanse at San Diego Supercomputer Center through allocation CTS120055 from the Advanced Cyberinfrastructure Coordination Ecosystem: Services & Support (ACCESS) program, which is supported by NSF grants # OAC-2138259, # OAC-2138286, # OAC-2138307, # OAC-2137603, and # OAC-2138296. This work was authored in part by the National Renewable Energy Laboratory, operated by Alliance for Sustainable Energy, LLC, for the US Department of Energy (DOE) under contract no. DE-AC36-08GO28308. Funding is provided by the US Department of Energy, the Office of Energy Efficiency and Renewable Energy, the Advanced Materials & Manufacturing Technologies Office (AMMTO), and the Bioenergy Technologies Office (BETO). This work was performed as part of the Bio-Optimized Technologies to keep Thermoplastics out of Landfills and the Environment (BOTTLE) Consortium and was supported by AMMTO and BETO under contract no. DE-AC36-08GO28308 with the National Renewable Energy Laboratory (NREL), operated by Alliance for Sustainable Energy, LLC. The views expressed in the article do not necessarily represent the views of the DOE or the US Government. The US Government retains and the publisher, by accepting the article for publication, acknowledges that the US Government retains a nonexclusive, paid-up, irrevocable, worldwide license to publish or reproduce the published form of this work, or allow others to do so, for US Government purposes.

#### **AUTHOR CONTRIBUTIONS**

Conceptualization, L.Y., Y.K., and T.J.M.; material synthesis, L.Y., K.B., J.O.R., and Y.K.; experimental analysis, L.Y., K.B., and C.L.; DFT calculations, X.L., L.J.B., and Y.K.; writing - original draft, L.Y., X.L., and Y.K.; writing - review & editing, L.J.B., Y.K., and T.J.M.; funding acquisition, L.J.B. and T.J.M.

#### **DECLARATION OF INTERESTS**

The authors declare no competing interests.

Received: September 15, 2023 Revised: October 17, 2023 Accepted: October 31, 2023 Published: November 27, 2023

#### **REFERENCES**

- 1. Jehanno, C., Pérez-Madrigal, M.M., Demarteau, J., Sardon, H., and Dove, A.P. (2019). Organocatalysis for depolymerisation. Polym. Chem. 10, 172–186.
- 2. Coates, G.W., and Getzler, Y.D.Y.L. (2020). Chemical recycling to monomer for an ideal, circular polymer economy. Nat. Rev. Mater. 5, 501–516.
- 3. Chu, M., Liu, Y., Lou, X., Zhang, Q., and Chen, J. (2022). Rational design of chemical catalysis for plastic recycling. ACS Catal. 12, 4659–4679.
- 4. Bergmann, M., Almroth, B.C., Brander, S.M., Dey, T., Green, D.S., Gundogdu, S., Krieger, A., Wagner, M., and Walker, T.R. (2022). A global plastic treaty must cap production. Science 376, 469-470.
- 5. Law, K.L., and Narayan, R. (2021). Reducing environmental plastic pollution by designing polymer materials for managed end-of-life. Nat. Rev. Mater. 7, 104–116.
- 6. Geyer, R., Jambeck, J.R., and Law, K.L. (2017). Production, use, and fate of all plastics ever made. Sci. Adv. 3, e1700782.





- 7. (2020). Global Nylon market analysis and outlook 2020–2027. Nylon 6 volumes will reach 5.3 million tons by 2027, despite COVID-19 -. ResearchAndMarkets.com. https://www.businesswire.com/news/home/20200730005398/en/Global-Nylon-Market-Analysis-and-Outlook-2020-2027—Nylon-6-Volumes-Will-Reach-5.3-Million-Tons-by-2027-Despite-COVID-19—ResearchAndMarkets.com.
- Hole, G., and Hole, A.S. (2020). Improving recycling of textiles based on lessons from policies for other recyclable materials: A minireview. Sustain. Prod. Consumption 23, 42–51.
- Industry Agenda (2016). The New Plastics Economy Rethinking the future of plastics. https://www3.weforum.org/docs/ WEF\_The\_New\_Plastics\_Economy.pdf.
- Macfadyen, G., Huntington, T., and Cappell, R. (2009). Abandoned, lost or otherwise discarded fishing gear. UNEP Regional Seas Reports and Studies, No. 185; FAO Fisheries and Aquaculture Technical Paper, No. 523. Rome, UNEP/FAO.
- Chhabra, E. (2016). Recycling nylon is good for the planet – so why don't more companies do it?. The Guardian. https://www.theguardian. com/sustainable-business/2016/may/18/ recycling-nylon-bureo-patagonia-sustainableclothing.
- Lebreton, L., Slat, B., Ferrari, F., Sainte-Rose, B., Aitken, J., Marthouse, R., Hajbane, S., Cunsolo, S., Schwarz, A., Levivier, A., et al. (2018). Evidence that the Great Pacific Garbage Patch is rapidly accumulating plastic. Sci. Rep. 8, 4666.
- Nelms, S.E., Barnett, J., Brownlow, A., Davison, N.J., Deaville, R., Galloway, T.S., Lindeque, P.K., Santillo, D., and Godley, B.J. (2019). Microplastics in marine mammals stranded around the British coast: ubiquitous but transitory? Sci. Rep. 9, 1075.
- Matthies, P., and Seydl, W.F. (1986). History and development of Nylon 6. In High Performance Polymers: Their Origin and Development, R.B. Seymour and G.S. Kirshenbaum, eds. (Springer Netherlands), pp. 39–53.
- Textile Institute (2008). Polyesters and Polyamides, B.L. Deopura and R. Alagirusamy, eds. (CRC Press).
- Cywar, R.M., Rorrer, N.A., Mayes, H.B., Maurya, A.K., Tassone, C.J., Beckham, G.T., and Chen, E.Y.-X. (2022). Redesigned hybrid nylons with optical clarity and chemical recyclability. J. Am. Chem. Soc. 144, 5366–5376.
- Nylon Market Size, Share (2029). Report|Global Industry Trends. https://www. fortunebusinessinsights.com/nylon-market-102007.
- Nylon Market Size (2022–2030). Share & Trends Report. https://www.grandviewresearch.com/ industry-analysis/nylon-6-6-market.
- Braun, M., Levy, A.B., and Sifniades, S. (1999). Recycling Nylon 6 carpet to caprolactam. Polym. Plast. Technol. Eng. 38, 471–484.
- Alberti, C., Figueira, R., Hofmann, M., Koschke, S., and Enthaler, S. (2019). Chemical recycling of end-of-life polyamide 6 via ring closing

- depolymerization. ChemistrySelect 4, 12638–12642.
- Nielsen, M., Jurasek, P., Hayashi, J., and Furimsky, E. (1995). Formation of toxic gases during pyrolysis of polyacrylonitrile and nylons. J. Anal. Appl. Pyrol. 35, 43–51.
- Lozano-González, M.J., Rodriguez-Hernandez, M.T., Gonzalez-De Los Santos, E.A., and Villalpando-Olmos, J. (2000). Physicalmechanical properties and morphological study on nylon-6 recycling by injection molding. J. Appl. Polym. Sci. 76, 851–858.
- 23. Bohnet, M. (2000). Ullmann's Encyclopedia of Industrial Chemistry, First Edition (Wiley).
- Bradford, S., Rupf, R., and Stucki, M. (2021). Climbing ropes—environmental hotspots in their life cycle and potentials for optimization. Sustainability 13, 707.
- Kamimura, A., and Yamamoto, S. (2007). An efficient method to depolymerize polyamide plastics: A new use of ionic liquids. Org. Lett. 9, 2533–2535.
- Yamamoto, S., and Kamimura, A. (2009). Preparation of novel functionalized ammonium salts that effectively catalyze depolymerization of Nylon-6 in ionic liquids. Chem. Lett. 38, 1016–1017.
- Kamimura, A., Shiramatsu, Y., and Kawamoto, T. (2019). Depolymerization of polyamide 6 in hydrophilic ionic liquids. Green Energy Environ. 4, 166–170.
- Kumar, A., von Wolff, N., Rauch, M., Zou, Y.-Q., Shmul, G., Ben-David, Y., Leitus, G., Avram, L., and Milstein, D. (2020). Hydrogenative depolymerization of nylons. J. Am. Chem. Soc. 142, 14267–14275.
- Ryu, J.-S., Marks, T.J., and McDonald, F.E. (2004). Organolanthanide-catalyzed intramolecular Hydroamination/Cyclization/ Bicyclization of sterically encumbered substrates. Scope, selectivity, and catalyst thermal stability for amine-tethered unactivated 1,2-Disubstituted alkenes. J. Org Chem. 69, 1038–1052.
- Hong, S., and Marks, T.J. (2004).
   Organolanthanide-catalyzed hydroamination.
   Acc. Chem. Res. 37, 673–686.
- Lide, D.R. (2005). Abundance of Elements in the Earth's Crust and in the Sea. In CRC Handbook of Chemistry and Physics (Internet Version), pp. 14–17.
- 32. Turekian, K.K., and Wedepohl, K.H. (1961).
  Distribution of the elements in some major units of the earth's crust. Geol. Soc. Am. Bull. 72, 175.
- Ruthenium price today|Historical ruthenium price charts|SMM metal market. https://www. metal.com/Other-Precious-Metals/ 201102250083.
- Eijsbouts, S., Anderson, G.H., Bergwerff, J.A., and Jacobi, S. (2013). Economic and technical impacts of replacing Co and Ni promotion in hydrotreating catalysts. Appl. Cat. A 458, 169–182.
- 35. Nuss, P., and Eckelman, M.J. (2014). Life cycle assessment of metals: A scientific synthesis. PLoS One 9, e101298.

- Wursthorn, L., Beckett, K., Rothbaum, J.O., Cywar, R.M., Lincoln, C., Kratish, Y., and Marks, T.J. (2023). Selective lanthanide-organic catalyzed depolymerization of Nylon-6 to e-caprolactam. Angew. Chem. Int. Ed. Engl. 62, e202212543.
- Jeske, G., Lauke, H., Mauermann, H., Swepston, P.N., Schumann, H., and Marks, T.J. (1985). Highly reactive organolanthanides. Systematic routes to and olefin chemistry of early and late bis(pentamethylcyclopentadienyl) 4f hydrocarbyl and hydride complexes. J. Am. Chem. Soc. 107, 8091–8103.
- 38. Jeske, G., Schock, L.E., Swepston, P.N., Schumann, H., and Marks, T.J. (1985). Highly reactive organolanthanides. Synthesis, chemistry, and structures of 4f hydrocarbyls and hydrides with chelating bis(polymethylcyclopentadienyl) ligands. J. Am. Chem. Soc. 107, 8103–8110.
- 39. Den Haan, K.H., De Boer, J.L., Teuben, J.H., Spek, A.L., Kojic-Prodic, B., Hays, G.R., and Huis, R. (1986). Synthesis of monomeric permethylyttrocene derivatives. The crystal structures of Cp<sub>2</sub>\*YN(SiMe<sub>3</sub>)<sub>2</sub> and Cp<sub>2</sub>\*YCH(SiMe<sub>3</sub>)<sub>2</sub>. Organometallics *5*, 1726–1733.
- Kosloski-Oh, S.C., Wood, Z.A., Manjarrez, Y., de los Rios, J.P., and Fieser, M.E. (2021). Catalytic methods for chemical recycling or upcycling of commercial polymers. Mater. Horiz. 8, 1084–1129.
- Mihut, C., Captain, D.K., Gadala-Maria, F., and Amiridis, M.D. (2001). Review: recycling of nylon from carpet waste. Polym. Eng. Sci. 41, 1457–1470
- 42. Amin, S.B., and Marks, T.J. (2008). Versatile pathways for in situ polyolefin functionalization with heteroatoms: catalytic chain transfer. Angew. Chem. Int. Ed. Engl. 47, 2006–2025.
- Schock, L.E., and Marks, T.J. (1988).
   Organometallic thermochemistry. Metal hydrocarbyl, hydride, halide, carbonyl, amide, and alkoxide bond enthalpy relationships and their implications in pentamethylcyclopentadienyl and cyclopentadienyl complexes of zirconium and hafnium. J. Am. Chem. Soc. 110, 7701–7715.
- 44. Booij, M., Meetsma, A., and Teuben, J.H. (1991). Ring hydrogen C-H activation in  $Cp^*_2LnCH(SiMe_3)_2$  (Ln = yttrium, lanthanum, cerium): x-ray crystal structures of  $[Cp^*_3(\mu_3-\eta_5,\eta^1,\eta^1-C_5Me_3(CH_2)_2)Ce_2]_2$  and  $Cp^*_2CeCH_2C_6H_5$ . Organometallics 10, 3246–3252.
- 45. Current prices for rare earths|Institute for Rare Earths and Metals Institut für Seltene Erden und strategische Metalle e.V. https://en.institut-seltene-erden.de/aktuelle-preise-vonseltenen-erden/.
- Moreira, A., Henriques, B., Leite, C., Libralato, G., Pereira, E., and Freitas, R. (2020). Potential impacts of lanthanum and yttrium through embryotoxicity assays with Crassostrea gigas. Ecol. Indic. 108, 105687.
- Li, Y., and Marks, T.J. (1996). Diverse mechanistic pathways and selectivities in organo-f-element-catalyzed hydroamination. Intermolecular Organolanthanide-catalyzed





- alkyne and alkene hydroamination. Organometallics 15, 3770–3772.
- Arredondo, V.M., Tian, S., McDonald, F.E., and Marks, T.J. (1999). Organolanthanide-catalyzed Hydroamination/Cyclization. Efficient allenebased transformations for the syntheses of naturally occurring alkaloids. J. Am. Chem. Soc. 121, 3633–3639.
- Green, J.C., and Jardine, C.N. (1999). Thermal stability of Group 6 bis(cyclopentadienyl) and ethylene bridged bis(cyclopentadienyl) monocarbonyl complexes; a theoretical study. J. Chem. Soc. Dalton Trans. 21, 3767–3770.
- Gagne, M.R., Stern, C.L., and Marks, T.J. (1992). Organolanthanide-catalyzed hydroamination. A kinetic, mechanistic, and diastereoselectivity study of the cyclization of N-unprotected amino olefins. J. Am. Chem. Soc. 114, 275–294.
- Falivene, L., Cao, Z., Petta, A., Serra, L., Poater, A., Oliva, R., Scarano, V., and Cavallo, L. (2019). Towards the online computer-aided design of catalytic pockets. Nat. Chem. 11, 872–879.
- 52. Carpet product stewardship|US EPA. https://archive.epa.gov/wastes/conserve/tools/stewardship/web/html/carpet.html.
- Ruggeri, C. (2022). The environmental impact of recycling carpet | Magazine Aquafil group. Aquafil. https://www.aquafil.com/magazine/ the-environmental-impact-of-recyclingcarpet/.
- Peng, Y., Wu, P., Schartup, A.T., and Zhang, Y. (2021). Plastic waste release caused by COVID-19 and its fate in the global ocean. Proc. Natl. Acad. Sci. USA 118, e2111530118.
- Bialas, D., Kirchner, E., Röhr, M.I.S., and Würthner, F. (2021). Perspectives in dye chemistry: A rational approach toward functional materials by understanding the

- aggregate state. J. Am. Chem. Soc. 143, 4500–4518.
- Schock, L.E., Brock, C.P., and Marks, T.J. (1987). Intramolecular thermolytic C-H activation processes. Solid-state structural characterization of a mononuclear η<sup>6</sup>-Me<sub>4</sub>C<sub>5</sub>CH<sub>2</sub> zirconium complex and a mechanistic study of its formation from (Me<sub>5</sub>C<sub>5</sub>)2Zr(C<sub>6</sub>H<sub>5</sub>)2. Organometallics 6, 232–241
- 57. Neese, F. (2012). The ORCA program system. WIREs Comp. Mol. Sci. 2, 73–78.
- Neese, F., Wennmohs, F., Becker, U., and Riplinger, C. (2020). The ORCA quantum chemistry program package. J. Chem. Phys. 152, 224108.
- Perdew, J.P., Ernzerhof, M., and Burke, K. (1996). Rationale for mixing exact exchange with density functional approximations. J. Chem. Phys. 105, 9982–9985.
- Adamo, C., and Barone, V. (1999). Toward reliable density functional methods without adjustable parameters: the PBEO model. J. Chem. Phys. 110, 6158–6170.
- Schäfer, A., Horn, H., and Ahlrichs, R. (1992). Fully optimized contracted Gaussian basis sets for atoms Li to Kr. J. Chem. Phys. 97, 2571–2577.
- 62. Weigend, F., and Ahlrichs, R. (2005). Balanced basis sets of split valence, triple zeta valence and quadruple zeta valence quality for H to Rn: design and assessment of accuracy. Phys. Chem. Chem. Phys. 7, 3297–3305.
- Grimme, S., Antony, J., Ehrlich, S., and Krieg, H. (2010). A consistent and accurate ab initio parametrization of density functional dispersion correction (DFT-D) for the 94 elements H-Pu. J. Chem. Phys. 132, 154104.

- Grimme, S., Ehrlich, S., and Goerigk, L. (2011). Effect of the damping function in dispersion corrected density functional theory. J. Comp. Chem. 32, 1456–1465.
- 65. Marenich, A.V., Cramer, C.J., and Truhlar, D.G. (2009). Universal solvation model based on solute electron density and on a continuum model of the solvent defined by the bulk dielectric constant and atomic surface tensions. J. Phys. Chem. B 113, 6378–6396.
- Weigend, F. (2006). Accurate Coulomb-fitting basis sets for H to Rn. Phys. Chem. Chem. Phys. 8, 1057–1065.
- 67. Neese, F., Wennmohs, F., Hansen, A., and Becker, U. (2009). Efficient, approximate and parallel Hartree–Fock and hybrid DFT calculations. A 'chain-of-spheres' algorithm for the Hartree–Fock exchange. Chem. Phys. 356, 98–109.
- Chemcraft Graphical program for visualization of quantum chemistry computations. https://www.chemcraftprog. com/.
- Pracht, P., Bohle, F., and Grimme, S. (2020). Automated exploration of the low-energy chemical space with fast quantum chemical methods. Phys. Chem. Chem. Phys. 22, 7169–7192.
- Lu, T., and Chen, Q. (2021). Shermo: A general code for calculating molecular thermochemistry properties. Comp. Theor. Chem. 1200, 113249.
- Grimme, S. (2012). Supramolecular binding thermodynamics by dispersion-corrected density functional theory. Chemistry 18, 9955–9964.
- Lu, T. (2022). Concvar: a computer program for simulating concentration variation of complex chemical reactions (Chemistry).